Journal of Nuclear Materials 509 (2018) 267–275

Contents lists available at ScienceDirect

Journal of Nuclear Materials

journal homepage: www.elsevier.com/locate/jnucmat

Microstructure and property tailoring of castable nanostructured alloys through thermomechanical treatments☆

L. Tan*, C.M. Parish, X. Hu

Oak Ridge National Laboratory, Oak Ridge, TN, 37831, United States

ARTICLE INFO

Article history:
Received 30 April 2018
Received in revised form
5 July 2018
Accepted 6 July 2018
Available online 6 July 2018

Keywords:
Tempered martensite
Ferrite
Dual-phase
Mechanical properties
Helium desorption

ABSTRACT

Three types of microstructures, i.e., tempered-martensite (TM), ferrite (F), and dual-phase (TM + F), were developed in a castable nanostructured alloy that favors a high density of nanoprecipitates compared with the precipitates in current reduced-activation ferritic-martensitic steels. The effect of the distinct microstructures on tensile properties, Charpy impact toughness, and thermal helium desorption behavior was investigated with the full TM structure as a reference. The results indicated that the F domain in the TM + F structure governed the strength and slightly impaired the impact toughness. The full F structure exhibited the highest strength without compromising ductility, but it noticeably diminished impact toughness. All microstructures had a dominant helium desorption peak at ~1070 °C. The higher density of nanoprecipitates and complex boundaries and dislocations in the TM + F structure enhanced the secondary helium desorption peak and extended the shoulder peak, in contrast to the full TM structure with an enlarged desorption peak associated with the ferrite-to-austenite transformation at ~810–850 °C and the full F structure with a dominant desorption peak related to bubble migration at ~1070 °C. These results suggest that components fabricated from functionally graded microstructures could be engineered to exploit the advantages of different microstructures for demanding application requirements.

1. Introduction

Current reduced-activation ferritic-martensitic (RAFM) steels, such as F82H and Eurofer97, have yield strengths similar to but creep strengths noticeably inferior to those of Grade 91 ferritic-martensitic (FM) steel [1,2]. The difference is attributable to the significantly lower amounts of nanoprecipitates in current RAFM steels [1], which are insufficient to pin the lath boundaries during recovery processes at temperatures above 600–650 °C. To produce advanced RAFM steels for future fusion energy applications, a variety of approaches have been explored and developed, primarily including alloy composition adjustment and thermomechanical treatments [2,3].

Castable nanostructured alloys (CNAs) are among the successful examples exploiting composition adjustment that are being developed as a new generation of RAFM steels. They favor the formation of high-density, stable MX (M = metal, X = C/N) nanoprecipitates and are produced using the same traditional steelmaking technologies as the current RAFM steels [1]. Increased amounts of MX nanoprecipitates—together with refinements in overall microstructure such as the sizes of laths, blocks, packets, and prior-austenite grains—have demonstrated different levels of improvements in tensile strength, creep resistance, Charpy impact toughness, and helium management [1,4]. The benefits of adding titanium in the CNAs were also observed in a recent study, which led to accelerated formation kinetics of (Ti,Ta)-rich MX and greater stability of the MX under thermal exposure [5]. Thermomechanical treatments have been broadly employed to engineer specific microstructures for desired properties. The goal of this study is to produce different base microstructures, i.e., full tempered martensite (TM), full ferrite (F), and dual-phase TM + F, by

☆ Notice: This manuscript has been authored by UT-Battelle, LLC, under contract DE-AC05-00OR22725 with the US Department of Energy (DOE). The US government retains and the publisher, by accepting the article for publication, acknowledges that the US government retains a nonexclusive, paid-up, irrevocable, worldwide license to publish or reproduce the published form of this manuscript, or allow others to do so, for US government purposes. DOE will provide public access to these results of federally sponsored research in accordance with the DOE Public Access Plan (http://energy.gov/downloads/doe-public-access-plan).

* Corresponding author. One Bethel Valley Road, P.O. Box 2008, MS-6136, Oak Ridge, TN, 37831, United States.
E-mail address: tanl@ornl.gov (L. Tan).

https://doi.org/10.1016/j.jnucmat.2018.07.012
0022-3115/

thermomechanical treatment of a CNA to examine the effects of the distinct microstructures on the mechanical properties and thermal helium desorption behavior. The results will provide essential insight for the microstructural design of RAFM steels and/or components with graded microstructures to meet diverse application requirements.

2. Experimental

A CNA with the composition Fe-8.6Cr-1.3W-0.6Mn-0.15V-0.1Ta-0.1Ti-0.1Si-0.13C-0.003 N in weight percent was cast by vacuum induction melting (VIM). The ingot was forged to form 41 mm thick plates, followed by normalization at 1130 °C for 2 h, rolling at high (>900 °C) or moderate (~700 °C) temperatures for 3 passes to achieve the same amount of thickness reduction (~32%), water quenching, and finally tempering at 750 °C for 2 h with air cooling. The materials generated under these two rolling conditions were called R900 and R700, respectively. The third condition was annealing at 980 °C for 0.5 h followed by furnace cooling (FC) after the 1130 °C/2 h normalization and water quenching. The processing procedures used for the three conditions of R900, R700, and FC are schematically illustrated in Fig. 1 and are characterized as TM, TM + F, and F microstructures, respectively, as presented in the following section.

Conventional mechanical grinding and polishing to a mirror finish were carried out to prepare metallographic samples of the materials produced under the three conditions for scanning electron microscopy (SEM: JEOL JSM-6500 F) characterization at 20 keV. Focused-ion beam (FIB) milling was used to prepare electron-transparent lamellae, followed by processing with Nano-Mill to mitigate FIB-generated artifacts for transmission electron microscopy (TEM: FEI Talos F200X and JEOL JEM-2100 F) characterization at 200 keV, primarily using scanning TEM (STEM) mode. Specimen thickness at the characterization regions was estimated using the convergent beam electron diffraction technique [6] for statistical quantitative analyses of dislocations and precipitates from two images per material condition. Energy dispersive x-ray spectroscopy (EDS) was employed for elemental mapping.

Vickers microhardness measurements were performed at room temperature with five measurements per material condition. Tensile tests were conducted using type SS-3 ($7.62 \times 1.52 \times 0.76$ mm gauge section) miniature specimens at a strain rate of 1×10^{-3} s^{-1} and temperatures of up to 800 °C. They were carried out with one test per material condition per temperature. Half-size Charpy impact specimens ($5 \times 5 \times 25.4$ mm with 1 mm deep V-notch), in a T–L (transverse–longitudinal) specimen orientation with the crack plane parallel to the longitudinal (i.e., rolling) direction, were tested to determine the upper-shelf energy (USE) and ductile-brittle transition temperature (DBTT). The thermal helium desorption behavior of the three alloy conditions was assessed by measuring the helium release flux (/cm^2/s) during sample heating at a ramping rate of 0.5 °C/s to a maximum temperature of 1300 °C after 10 keV helium ion injection of 5×10^{15} cm^{-2} into the surface-mirror–finished samples.

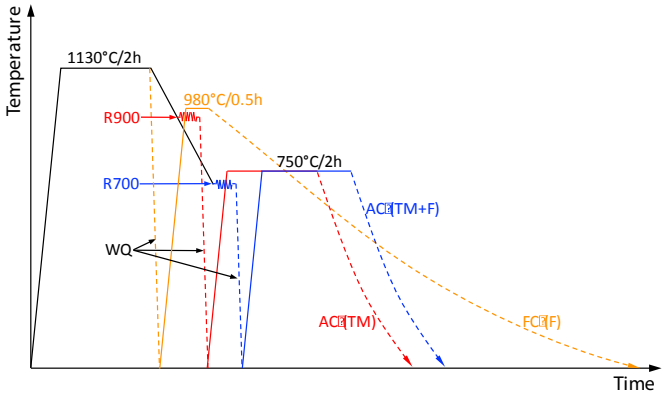

Fig. 1. Processing procedures to obtain three material conditions of a CNA, identified as R900, R700, and FC in red, blue, and orange, respectively for better visualization. (For interpretation of the references to colour in this figure legend, the reader is referred to the Web version of this article.)

3. Results and discussion

3.1. Microstructures

Computational thermodynamics was employed to calculate the equilibrium phase stability and composition, which help understand the microstructure of the alloy at an equilibrium state. Fig. 2 plots the temperature-dependent phase mole fraction and the compositions of the primary precipitates, calculated using the JMatPro Fe-alloy database. Fig. 2a indicates MX precipitates in two forms of Ti(C,N) (Fig. 2b) and (Ti,Ta)C (Fig. 2c), together with Cr-rich $M_{23}C_6$ (Fig. 2d), in the matrix experiencing liquid, δ-ferrite, γ-austenite, and α-ferrite phases as temperature decreases. Laves phase would not be observed in the as-fabricated alloys because of its sluggish formation [7]. The nitrogen content (0.003 N) was controlled as low as possible to favor primarily carbides formation in the CNA as suggested in Fig. 2a. The nitrogen content is nearly one order of magnitude lower than that in F82H (~0.01 N) and Eurofer97 (~0.02 N) or recently modified Eurofer97 (>0.04 N [8]). The CNA with primarily Ti/Ta-rich carbides contrasts with the nitrogen-alloyed RAFM steels with primarily V/Ta-rich carbonitrides [8].

The backscattered electron (BSE) images of the R900, R700, and FC samples, the three conditions of a CNA, characterized by SEM are shown in Fig. 3, which reveal crystallographic and atomic number contrast. Whereas the R900 in Fig. 3a has a full TM microstructure with a prior-austenite grain (schematically outlined by dashed blue lines) size on the order of 50 μm, the R700 in Fig. 3b contains a dual-phase microstructure with TM as the dominant matrix structure, together with a network of fine-grained (~2 μm) F filling an ~32% area fraction. The TM domains in light gray, surrounded by the F grain network in dark gray, have sizes ranging from ~10 to ~20 μm. It is believed that the F grains were formed at the prior-austenite and martensite-packet boundaries during the rolling at 700 °C. In contrast, as shown in Fig. 3c, only F was observed in the FC sample, which had a grain size on the order of 20 μm. The insets in Fig. 3 show BSE images at a higher magnification, revealing many white precipitates in a size range of ~70–250 nm. The white particles are believed to be tantalum (Ta) -rich MX-type precipitates, identified by EDS as well as by the high atomic mass of Ta for the contrast in the BSE images. It is believed that the Ta-rich MX is (Ti,Ta)C according to Fig. 2, which was formed during normalization. The generally larger particles in the R900 sample are attributable to coarsening during rolling at 900 °C. The rolling at 700 °C might have partially destabilized the Ta-rich MX because of the decreased fraction of (Ti,Ta)C in Fig. 2a at temperatures below ~830 °C, leading to slightly smaller particles in R700. The TM (lower right) in the dual-phase microstructure appears to have an area number density of white particles similar to that of the F grains (top left) as shown in the inset of Fig. 3b. The second brief normalization at 980 °C followed by FC resulted in relatively small particles with a minimal deviation in the FC sample (Fig. 3c). Given the same SEM voltage and work-distance during the characterization, the area number density of the white particles is 0.78, 0.59, and 0.97 μm^{-2} in the